Available online at www.sciencedirect.com

ScienceDirect

Physics Procedia 83 (2016) 36 – 45

Physics Procedia

9th International Conference on Photonic Technologies - LANE 2016

Synthesis and characterization of Pd nanoparticles by laser ablation in water using nanosecond laser

M. Boutinguiza[a], M. Meixus[a], J. del Val[a], A. Riveiro[a] R. Comesaña[b], F. Lusquiños[a], J. Pou[a,*]

[a]*Applied Physics Department, University of Vigo, EEI, Lagoas-Marcosende, 36310 Vigo, Spain*
[b]*Materials Engineering, Applied Mechanics and Construction Department, University of Vigo, EEI, 36310 Vigo, Spain*

Abstract

Colloidal solutions of Pd nanoparticles were produced by laser ablation of solids in liquids (LASL) technique. Two different lasers operating at 1064 and 532 nm of wavelength to ablate a Pd foil submerged in water were used. The properties of the obtained nanoparticles were studied and the influence of the wavelength on the nanoparticle size was discussed. The nanoparticles formation mechanism is discussed and compared with the results obtained in previous work using continuous wave (CW) and long pulses lasers. The obtained nanoparticles were characterized by means of transmission electron microscopy (TEM), high resolution transmission electron microscopy (HRTEM) and UV/VIS absorption spectroscopy. The obtained nanoparticles consisted of crystalline Pd nanoparticles with rounded shape and strong tendency to agglomeration. The size distribution of the nanoparticle range from few nanometers to 40 nm together with the presence of occasional large particles when the infrarred (IR) laser was used.

Peer-review under responsibility of the Bayerisches Laserzentrum GmbH

Keywords: laser ablation; palladium nanoparticles; nanosecond laser

1. Introduction

Nanomaterials having one or more dimensions in the range of 1-100 nm are considered a bridge between the atomic and bulk materials which is revolutionizing science, technology and industry, thanks to the phenomena related to the increased surface to volume ratio. In the last decades metal noble nanoparticles such as Au, Ag, Pd,

* Corresponding author. Tel.: +34-986812216 ; fax: +34-986812201 .
E-mail address: jpou@uvigo.es

Peer-review under responsibility of the Bayerisches Laserzentrum GmbH
doi:10.1016/j.phpro.2016.08.005

etc. have attracted attention of researchers due to their unique physical, chemical and electronical properties obtainable at nanoscale, different from that of bulk material (see Krutyakov et al. (2008), Menéndez-Manjón et al. (2011), or Boutinguiza et al. (2015)).

Pd is a transition metal with the lowest melting point and the lowest density of the platinum group of metals, showing interesting characteristics such as stable electrical properties, high resistance to wear, and exceptional catalytic properties. These properties make palladium a very appealing material being used mainly as catalyst in lots of processes (see the review by Astruc et al. (2005)). In particular the novel properties of Pd nanoparticles encouraged investigations in many different fields, among them nano-catalysis, fuel cells by the use of Pd as hydrogen storage, sensors, etc. Hamasaki et al. (2014) used Pd nanoparticles with a Co3O4 support for the formulation of aryl iodides. Nair et al. (2015) demonstrated the capabilities of Pd nanoparticles to enhance hydrogen storage when using nitrogen rich carbon material and Mijowska et al. (2015) used Pd nanoparticles in an electrochemical enzymatic biosensor to detect glucose.

There are a lot of different techniques and methods for producing Pd nanoparticles and nanostructured Pd based materials which can be classified in chemical and physical groups. Chemical reduction which typically uses reducing agents to generate nanoparticle with different sizes and composition; for instance Nguyen et al (2010) synthesized Pd nanoparticles with different shapes and sized by polyol method. Hydrothermal method is an easy and low cost technique for producing nanoparticles and enables altering the crystalline structure and the composition of the resulted particles by adjusting parameters such as temperature, pressure, or precursor concentration. Chang et al. (2009) obtained ZnO modified with various contents of Pd through hydrothermal method. However, many of these techniques use precursors and solvents, or imply chemical reactions which can contaminate the obtained nanoparticles, besides the lack of stability of the obtained product as well as low uniformity and dispersivity of the nanoparticles.

Physical techniques involve the use of precursor metals to obtain nanomaterials without the formation of new substances, but by the molecular rearrangement. Different physical techniques have been used to produce Pd films and Pd nanoparticles. Joshi et al. (2009) reported the use of Pd nanoparticles obtained by sputtering for hydrogen detection, while Slavcheva et al. (2014) reported the physical and electrochemical characterization of Pd films obtained by sputtering. Among the wide spectrum range of physical methods, LASL has emerged last years as an efficient technique in the generation of metal nanoparticles due to chief advantages like obtaining stable and dispersed nanoparticles and nanocolloids together with the absence of contaminants. Cristoforetti et al. (2012, 2013) obtained and characterized Pd nanoparticles in water and other organic solvent using pulsed laser, while Nishi et al. (2013) reported the preparation of monodispersed Pd nanoparticles at the water-air interface using pulsed laser. Marzuna et al. (2015) controlled the size of the nanoparticles by using a saline solution. In previous work we had explored synthesizing crystalline nanoparticles using continuous wave (CW) laser as well as millisecond pulsed laser, Boutinguiza et al. (2014). In the present work we report the results of an experimental work devoted to obtain Pd nanoparticles by laser ablation of a palladium target in water using nano and picosecond lasers with different wavelengths.

2. Materials and methods

Palladium foils with 99.99% of purity were cleaned and sonicated to be used as laser ablation targets. The foils were fixed to a bottom of a glass vessel and filled with milli-Q water up to 1 mm over the upper surface of the Pd foil (more details can be found in Boutinguiza et al. 2011a). Two different lasers sources have been used to ablate the targets. First system was a diode-pumped Nd:YVO_4 laser providing pulses at wavelength of 532 nm, 0,30 mJ of pulse energy and pulse duration of 10 ns; while the second laser source consisted of a picosecond diode-pumped Nd:YVO_4 laser delivering pulses at 1064 nm of wavelength, 800 ps of duration and 0.03 mJ of pulse energy. Processing parameters used with both lasers are listed in table 1. In all experiments laser beam was focused on the upper surface of the target to give a fluence of 0.2 to 2 J/cm^2, and was kept in relative movement with respect to the metallic plate at 5 mm/s of scanning speed in the case of nanosecond laser and at 20 and 40 mm/s when the picosecond laser was used These conditions enabled similar overlapping for both lasers with similar interpulse distances, 0.25 μm in the case of nanosecond laser and 0.10 and 0.20 μm for the picosecond laser. The processing

time for the tests, considered as the time taken to get the solution coloured, was 11 minutes when using the nanosecond laser and 11 minutes when using the picosecond one.

Samples of colloidal solutions were deposited on Si substrates and on coated copper microgrids and allowed to dry for characterization. Scanning electron microscopy (SEM) was used to observe and analyze the surface morphology and the microstructure by means of a JEOL JSM-6700 field emission scanning electron microscope. Transmission electron microscopy (TEM), selected area electron diffraction (SAED) and high-resolution transmission electron microscopy (HRTEM) images were taken on a JEOL-JEM 2010 FEG transmission electron microscope equipped with a slow digital camera scan, using an accelerating voltage of 200 kV, and provided with an energy dispersive X-ray spectrometer (EDS) to reveal their crystallinity and composition. The optical absorption by palladium nanoparticles in colloidal solutions was measured by U-vis Hewlett Packard HP 8452 spectrophotometer at the wavelength range of 190-800 nm in a 10 mm quartz cell. Electron energy loss spectroscopy (EELS) was carried out in order to check the potential presence of oxygen in the nanoparticles.

Table 1. Laser sources and their corresponding parameters.

Laser source	Wavelength (nm)	Pulse length (ns)	Frequency (kHz)	Average power (W)	Scanning speed (mm/s)
Nanosecond laser	532	10	20	6.0	5.0
Picosecond laser	1064	0.8	200	6.0	20

3. Results and discussion

The morphology, composition and crystalline structure of the obtained nanoparticles have been studied by SEM, TEM and HRTEM. Figures 1 and 2 show TEM images of nanoparticles obtained under 532 and 1064 wavelengths. Note that even when different laser parameters were used during processing with the different laser sources, the laser irradiance is similar in both cases (10^8 W/cm^2 aprox.), since the spot size and the average power (6 W) were similar. The appearances as well as the sizes of the obtained nanoparticles in present work are different from that obtained in previous work by the use of CW and millisecond lasers (see Boutinguiza et al. 2011b, 2014), showing larger sizes and low ablation rate than those obtained in the present work. This is due to the formation mechanism of nanoparticles and the regime taking place between laser beam and the target. When CW or long pulse (millisecond range) laser beam strikes on the Pd target, the incident radiation is absorbed heating up the palladium target above its melting point. At the same time, a very thin layer of liquid surrounding the droplets is evaporated, which can react with the droplets to give the final particles.

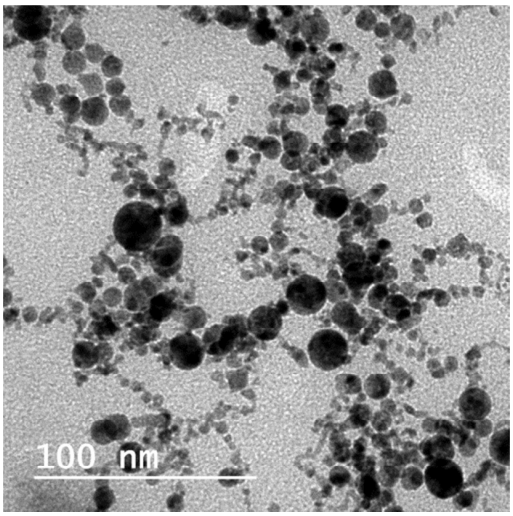

Fig. 1. Pd nanoparticles obtained by laser ablation of Pd foil in water using a pulsed laser operating at 532 nm.

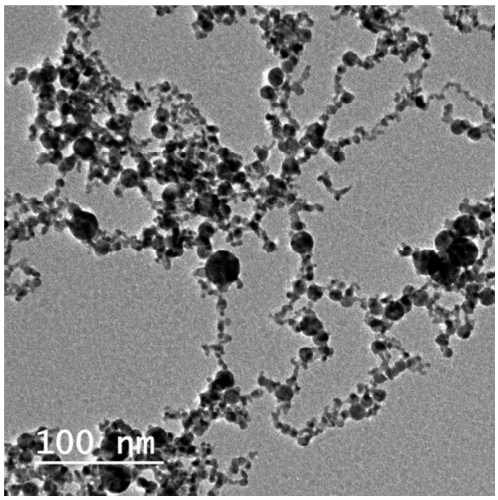

Fig. 2. Pd nanoparticles obtained by laser ablation of Pd foil in water using a pulsed laser operating at 1064 nm.

As temperature of the target is lower in the case of using long pulse laser than when short pulses (nanosecond range or shorter pulses) are used, explosive boiling takes place leading to the nanoparticle formation by means of nanodroplets rather than plasma. When long pulses are used, the nanoparticles are mainly formed by nanodroplets which are ejected into the surrounding liquid at very high speed. In the present work the nanoparticle formation mechanism is different. The use of laser pulses with nanosecond and picosecond duration under the aforementioned laser intensity, enable the formation of a plume (Liu et al., 2008). Different species such as atoms, ions and droplets are confined by the surrounding liquid to nucleate and grow by coalescence during the plasma cooling (Yang et al., 2007) to form the final nanoparticles. In our results the nanoparticles show a clear tendency to agglomeration, forming web like clusters in some cases. According to the results of works reported by Sakka et al., (2000) and Yang et al, (2007), ablation starts a few picoseconds after laser irradiation. In the case of nanosecond pulse lasers, the plasma expansion lasts more time than the duration of the pulse, leading to overlapping between the ablated material and the pulses. This effect could partially explain the wide range of nanoparticle sizes as well as the strong tendency to coalescence observed in particles

obtained by both wavelengths. Particle size reduction could also take place as observed in previous works (Boutinguiza et al. 2009). Nevertheless when the IR laser with pulse laser duration one order of magnitude shorter than that of the green laser was used, more presence of larger particles have been observed as can be seen from the figures 1 and 2 as well as is depicted in the histograms in figures 3 and 4 including the mean diameter and the standard deviation. The histograms have been obtained by measuring the dimensions of more than 500 nanoparticles for each case. By measuring the target weight before and after the tests together with the processing time, we have obtained ablation rates of 7.1 mg/h and 24 mg/h for nanosecond and picosecond laser respectively. This result can be considered as a high ablation rate when compared with others obtained with similar lasers (Cristoforetti et al.2011)

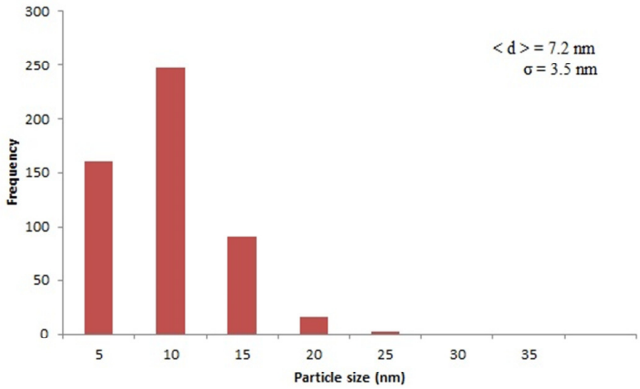

Fig. 3. Histogram of more than 500 particles obtained by laser ablation of Pd in water using a pulsed laser operating at 532 nm.

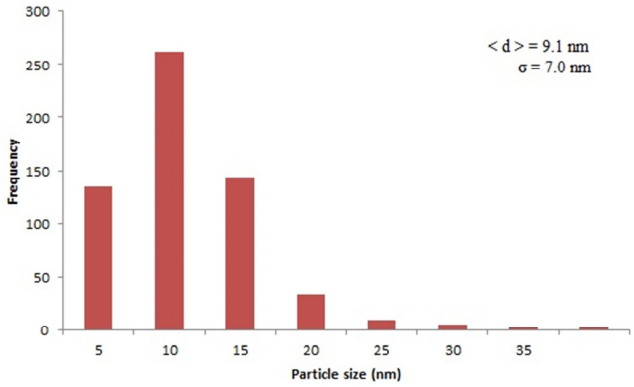

Fig. 4. Histogram of more than 500 particles obtained by laser ablation of Pd in water using a pulsed laser operating at 1064 nm.

The particle mean size is similar in both cases, being the presence of the occasional large particles more frequent when the infrared wavelength was used. This could be explained by the relatively low photon energy of infrared wavelength and the plasma formation by inverse Bremsstrahlung effect, which is considerably favorable of infrared wavelengths than for lower wavelengths (Russo et al., 2000). This contributes to increase the temperature of plasma and favoring the formation of larger nanoparticles, as is also reported by Kim et al. (2014). The morphology and the sizes of nanoparticles are crucial aspects that govern their properties and consequently their performance in many different applications. Assuming the spherical shape for the nanoparticles and considering their reduced mean diameters, the obtained Pd nanoparticles in this work exhibit very high specific surface area, which is crucial aspect,

especially taking into account that Pd is widely used in many energy and environmental activities. But they are limited by their low dispersivity due to their strong tendency to agglomeration.

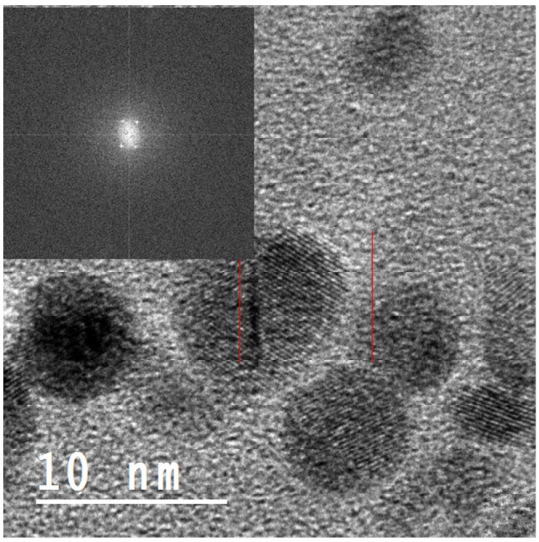

Fig. 5. HRTEM image of a single crystalline Pd nanoparticle obtained by laser ablation in water using pulsed laser operating at 532 nm and its corresponding FFT (inset). The measured lattice plane spacing (0.225 nm) can be assigned to that of Pd (0.225 nm).

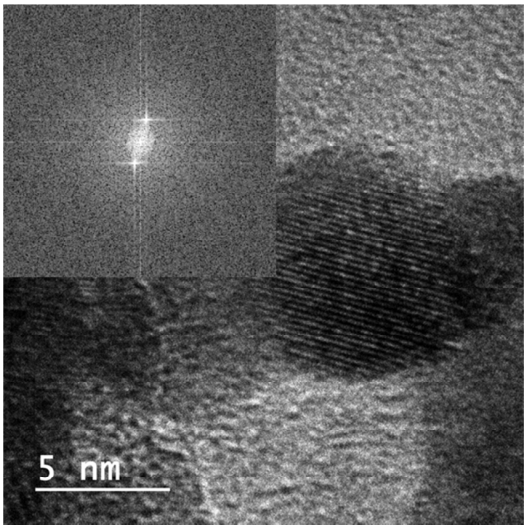

Fig. 6. HRTEM image of a single crystalline Pd nanoparticle obtained by laser ablation in water using pulsed laser operating at 1064 nm and its corresponding FFT (inset). The measured lattice plane spacieng (0.223 nm) matchs the one of Pd (0.225 nm).

All the particles obtained under the conditions mentioned before using both lasers are crystalline. This aspect can be observed in figures 5 and 6, showing HRTEM of single nanoparticles obtained by 532 and 1064 nm respectively and their corresponding Fast Fourier Transform (FFT) as insets. The measured lattice plane spacing for figure 5 is 0.225 nm

while for the figure 6 is 0.223 nm, which could be assigned to the {111} family planes of metallic Pd with cubic lattice spacing of 0.225 nm. To better elucidate the crystalline phases of both groups of nanoparticles SAED was performed on several groups of particles as shown in figures 7 and 8. The measured interplanar distances from 7 and 8 are listed in tables 2 and 3 respectively and compared with their corresponding of Pd. Despite the well agreement between the measured interplanar distances with those of cubic metallic Pd, as well as the stability and the low reactivity of Pd, the presence of oxygen could not be completely excluded. The formation of Pd nanoparticles takes place at high temperature and in the presence of species from the plasma plume including O_2 and H_2 coming from the evaporated water.

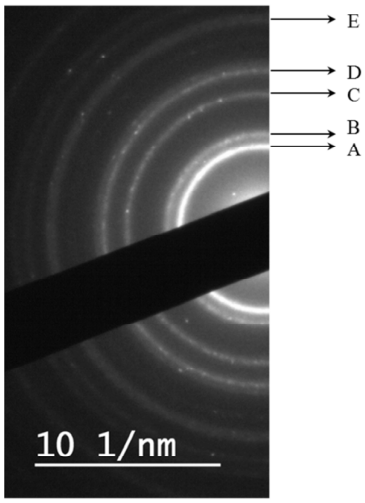

Fig. 7. SAED pattern obtained over a group of Pd nanoparticles obtained by the use of a pulsed laser operating at 532 nm. The interplanar distances of the main reflections are compared with those of crystalline Pd in table 2.

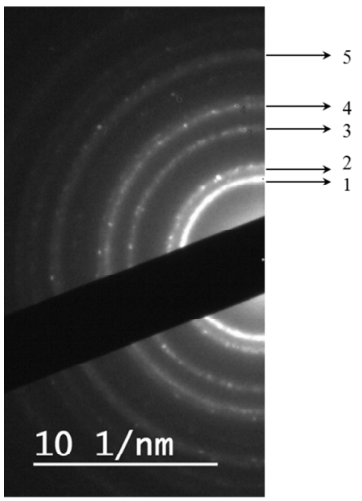

Fig. 8. SAED pattern obtained over a group of Pd nanoparticles obtained by the use of a pulsed laser operating at 1064 nm. The interplanar distances of the main reflections are compared with those of crystalline Pd in table 3.

Table 2. Lattice spacing measured from SAED performed on Pd nanoparticles obtained in water using 532 nm laser compared to those of metallic Pd.

	A	B	C	D	E
Measured d_{hkl} (nm)	0.225	0.196	0.137	0.117	0.110
Pd (d_{hkl} nm) JCPDS_ICDD(1993)	0.225	0.195	0.138	0.117	0.112

Table 3. Lattice spacing measured from SAED performed on Pd nanoparticles obtained in water using 1064 nm laser compared to those of metallic Pd.

	1	2	3	4	5
Measured d_{hkl} (nm)	0.226	0.195	0.137	0.117	0.094
Pd (d_{hkl} nm) JCPDS_ICDD(1993)	0.225	0.195	0.138	0.117	0.097

In order to experimentally corroborate the presence of oxygen in the obtained nanoparticles, electron energy loss spectroscopy (EELS) analysis was carried out. The corresponging spectrum is depicted in figure 9, indicating a sligh peak around 540 eV, which could be assigned to the oxygen. This result suggests that the presence of oxygen could not be ruled out. The choice of different solvent such as acetone, could avoid the oxidation of nanoparticles besides producing monodisperse particle in this process. It is expected that the use organic solvent would enable the formation of metallic nanoparticles and avoid oxidation. Indeed, it has been reported that the use of organic solvents in LASL leads to the decomposition of solvent and promote the formation of amorphous carbon, which can passivate the obtained Pd nanoparticles as reported by De Bonis et al. (2014) and Semaltianos et al. (2013). But in some applications, such as photocatalysis or photovoltaic, the nanomaterial surface should be as clean as possible.

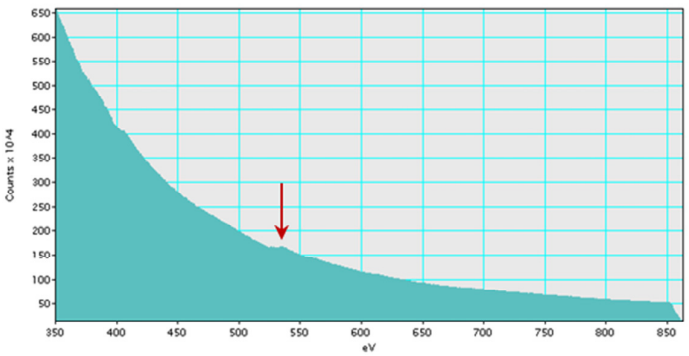

Fig. 9. EELS spectrum of Pd nanoparticle obtained by pulsed laser operating at 1064 nm. The peak around 540 eV indicated by the arrow can be assigned to oxygen.

The nanoparticles obtained in this work show no presence of contamination but partial oxidation has been observed in some particles, specially on the large ones. The presence of oxygen in the shell of the ejected droplets cannot be excluded, since the liquid layers surrounding the ejected droplets are rapidly evaporated due to the heat transmission from droplets to liquid, enabling this way the reaction between the shell of droplets and the evaporated water. This is in agreement with the results reported by Selmantianos et al. (2013). They observed the absence of phase-oxide in XRD spectra corresponding to Pd nanoparticles synthesised in deionized water, but oxides of Pd

were detected in their XPS indicating the partial surface oxidation of Pd nanoparticles.

The optical properties of the colloidal solutions obtained by both lasers are quite similar. Figure 10 shows UV-vis spectrum of colloidal solution obtained by the use of the pulsed laser operating at 532 nm which was similar to different solutions obtained under the experimental conditions mentioned above using 1064 as well as 532 nm wavelength laser.The spectrum shows a clear recognizable peak about 200 nm attributed to absorption of ionic Pd^{+2}, which is in agreement with the theoretical calculations for spherical nanoparticles of Pd based on the Mie theory as reported by Cárdenas-Triviño et al. (2004). There is no clear peak corresponding to the peak attributable to oxidized palladium species reported by De Bonis et al. (2014). Nevertheless in our case, the kind of shoulder extending towards higher wavelength until 290 nm could be due to the presence of oxidized species of Pd and/or agglomeration of nanoparticles.

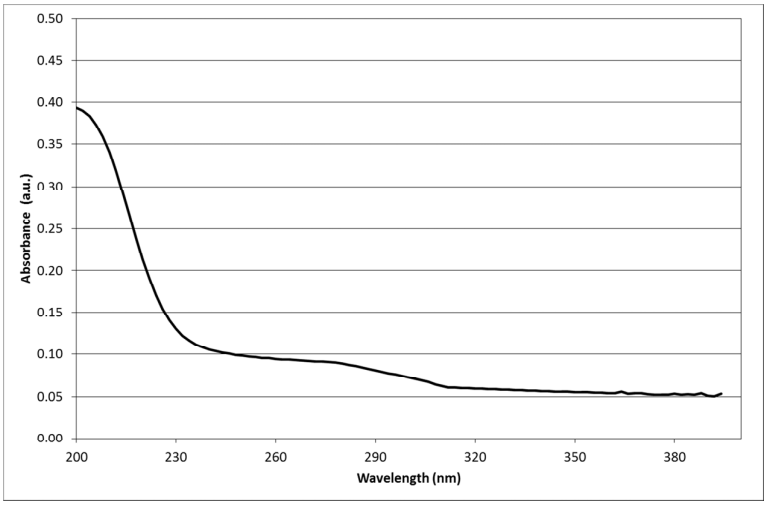

Fig. 10. Absorption spectrum of colloidal nanoparticles of Pd obtained by pulsed laser ablation of Pd foil in water using a pulsed laser operating at 532 nm.

4. Conclusions

Crystalline nanoparticles of Pd have been obtained by means of LASL technique using two different lasers operating at 532 and 1064 nm of wavelength without any chemical reagent or contamination. High rate of Pd nanoparticles can be obtained by both wavelengths at relatively low irradiance. The obtained particles exhibited reduced dimensions, ranging from few nanometers to 40 nm, with the exception of some occasional larger particles produced when IR laser was used, which could be attributed to the high temperature of plasma generated by the inverse Bremsstrahlung effect. All particles showed high specific surface area, but in all cases the obtained particles showed very strong tendency to agglomeration.

Acknowledgements

This work was partially supported by Government of Spain (MAT2015-71459-C2-P, Mobility Grant of Senior Professors and Researchers (Grant PRX15/00088)), and by Xunta de Galicia (CN2012/292, POS-A/2013/161). The authors wish to thank the technical staff from CACTI (University of Vigo) for their technical assistance.

References

Astruc, D., Lu, F., Aranzaes, J.R. (2005) Nanoparticles as recyclable catalysts: The frontier between homogeneous and heterogeneous catalysis. Angewandte Chemie 44 7852-7872.

Boutinguiza, M., Lusquiños, F., Riveiro, A., Comesaña, R., Pou, J. (2009). Hydroxylapatite nanoparticles obtained by fiber laser induced fracture. App. Surf. Sci. 255 5382-5385.

Boutinguiza, M., Pou, J., Lusquiños, F., Comesaña, R., Riveiro, A. (2011). Laser-assisted production of tricalcium phosphate nanoparticles from biological and synthetic hydroxyapatite in aqueous medium. App. Surf. Sci. 257 5195–5199.

Boutinguiza, M., Rodriguez-Gonzalez, B., del Val, J., Comesaña, R., Lusquiños, F., Pou, J. (2011). Laser-assisted production of spherical TiO_2 nanoparticles in water. Nanotechnology 22 195606.

Boutinguiza, M., Comesaña, R., Lusquiños, R., Riveiro, A., del Val, J., Pou, J., 2014. Palladium nanoparticles produced by CW and pulsed laser ablation in water. Applied Surface Science 302, 19-23.

Boutinguiza, M., Comesaña, R., Lusquiños, F., Riveiro, A., del Val, J., Pou, J. (2015) Production of silver nanoparticles by laser ablation in open air. App. Surf. Sci. 336 108–111.

Cárdenas-Triviño, G., Segura, R. A., Reyes-Gasga, J., 2004. Palladium nanoparticles from solvated atoms-stability and HRTEM characterization. Colloid. Polym. Sci. 282,1206–1212.

Chang, Y., Xu, J., Zhang, Y., Ma, S., Xin, L., Zhu, L., Xu, C., 2009. Optical Properties and Photocatalytic Performances of Pd Modified ZnO Samples. J. Phys. Chem. C 113, 18761–18767.

Cristoforetti, G., Pitzalis, E., Spiniello, R., Ishak, R., Muniz-Miranda, M., 2011 Production of palladium nanoparticles by pulsed laser ablation in water and their characterization. J. Phys. Chem. C 115, 5073−5083.

Cristoforetti, G., Pitzalis, E., Spiniello, R., Ishak, R., Giammanco, F., Muniz-Miranda, M., Caporali, S., 2012. Physico-chemical properties of Pd nanoparticles produced by pulsed laser ablation in different organic solvents. Appl. Surf. Sci. 258, 3289−3297.

De Bonis, A., Sansone, M., Galasso, A., Santagata, A., Teghil, R., 2014. The role of the solvent in the ultrashort laser ablation of palladium target in liquid. Appl. Phys. A 117, 211–216.

Hamasaki, A., Yasutake, H., Norio, T., Ishida,T., Akita, T., Ohashi, H., Yokoyama,T., Honma,T., Tokunaga, M.,2014. Cooperative catalysis of palladium nanoparticles and cobalt oxidesupport for formylation of aryl iodides under syngas atmosphere. Applied Catalysis A: General 469, 146– 152.

Joshi, R.K., Krishnan, S., Yoshimura, M., Kumar, A., 2009. Pd nanoparticles and thin films for room temperature hydrogen sensor. Nanoscale Res. Lett. 4, 1191–1196.

Kim, J., Reddy, D.A., Ma, R., Kim, T.K., 2014. The influence of laser wavelength and fluence on palladium nanoparticles produced by pulsed laser ablation in deionized water. Solid State Sciences 37, 96-102.

Krutyakov, Y.A., Kudrinskiy, A.A., Olenin, A.Y., Lisichkin, G.V. (2008) Synthesis and properties of silver nanoparticles: advances and prospects, Russ. Chem. Rev. 77 233–257.Nair, A.A.S., Sundara, R., Anitha, N., 2015. Hydrogen storage performance of palladium nanoparticles decorated graphitic carbon nitride. international journal o f hydrogen energy 40, 3259-3267.

Liu, P. S.; Cai, W. P.; Zeng, H. B., 2008. Fabrication and size-dependent optical properties of FeO nanoparticles induced by laser ablation in a liquid medium J. Phys. Chem. C 112, 3261–3266.

Marzuna, G., Nakamura, J., Zhang, X., Barcikowski, S., Wagener, P. (2015) Size control and supporting of palladium nanoparticles made by laser ablation in saline solution as a facile route to heterogeneous catalysts. App. Surf. Sci. 336 108–111.

Menéndez-Manjón, A., Barcikowski, S. (2011) Hydrodynamic size distribution of gold nanoparticles controlled by repetition rate during pulsed laser ablation in water. App. Surf. Sci. 257 4285-4290

Mijowska, E., Onyszkoa,M., Urbasa,K., Aleksandrzaka, M., Shia, X., Moszynski, D., Krzysztof, P., Podolskic, J., El Fray, M.,2015. Palladium nanoparticles deposited on graphene and its electrochemical performance for glucose sensing. Applied Surface Science 355, 587–592.

Nguyen, V.L., Nguyen, D.C., Hirata H., Ohtaki M., Hayakawa, T., Nogam, M., 2010. Chemical synthesis and characterization
of palladium nanoparticles. Advances in natural sciences: nanoscience and nanotechnology 1, 035012.

Nishi, T., Suzuki, N., Takahashi, N., Yano, K.,2013. Preparation of monodispersed Pd nanoparticles by laser ablation at air-suspension interface. J. Nanopart. Res., 15, 1−7.

Russo, R. E., Mao, X. L., Borisov, O. V., Liu, H., 2000. Influence of wavelength on fractionation in laser ablation ICP-MS. J. Anal. At. Spectrom. 15, 1115-1120.

Sakka, T., Iwanaga, S., Ogata, Y. H., Matsunawa, A., Takemoto, T., 2000. Laser ablation at solid–liquid interfaces: An approach from optical emission spectra. J. Chem. Phys.112, 8645–8653.

Semaltianos, N.G., Petko, P., Scholz, S., Guetaz L.,2013. Palladium or palladium hydride nanoparticles synthesized by laser ablation of a bulk palladium target in liquids. J. Colloid Interface Sci. 402, 307-311.

Slavcheva, E., Ganske, G., Schnakenberg, U., 2014. Sputtered Pd as hydrogen storage for a chip-integrated microenergy system. The Scientific World Journal. 2014, 146126.

Yang, G. W., 2007. Laser ablation in liquids: Applications in the synthesis of nanocrystals. Prog. Mater. Sci. 52, 648–698.